8-17-2020

Signals in the Soil: Underground Antennas

Abdul Salam
Purdue University, salama@purdue.edu

Usman Raza
Purdue University

Chapter 6
Signals in the Soil: Underground Antennas

Abstract Antenna is a major design component of Internet of Underground Things (IOUT) communication system. The use of antenna, in IOUT, differs from traditional communication in that it is buried in the soil. Therefore, one of the main challenges, in IOUT applications, is to establish a reliable communication. To that end, there is a need of designing an underground-specific antenna. Three major factors that can impact the performance of a buried antenna are: 1) effect of high soil permittivity changes the wavelength of EM waves, 2) variations in soil moisture with time affecting the permittivity of the soil, and 3) difference in how EM waves propagate during above-ground (AG) and underground (UG) communications. For the third challenge above, it to be noted that lateral waves are dominant component in EM during UG2UG communication and suffers lowest attenuation as compared to other, direct and reflected, components. Therefore, antennas used for over-the-air (OTA) communication will not be suitable for UG communication because of impedance mismatch. This chapter focuses on developing a theoretical model for understanding the impact of soil on antenna by conducting experiments in different soil types (silty clay loam, sandy, and silt loam soil) and indoor testbed. The purpose of the model is to predict UG antenna resonance for designing efficient communication system for IOUT. Based on the model a wideband planar antenna is designed considering soil dispersion and soil-air interface reflection effect which improves the communication range five times from the antennas designed only for the wavelength change in soil. Furthermore, it also focuses on developing an impedance model to study the effect of changing wavelength in underground communication. It is also discussed how soil-air interface and soil properties effect the return loss of dipole antenna.

6.1 Introduction

Antenna is a major design component of Internet of Underground Things (IOUT) communication system. This chapter focuses on developing a theoretical model for understanding the impact of soil on antenna by conducting experiments in different

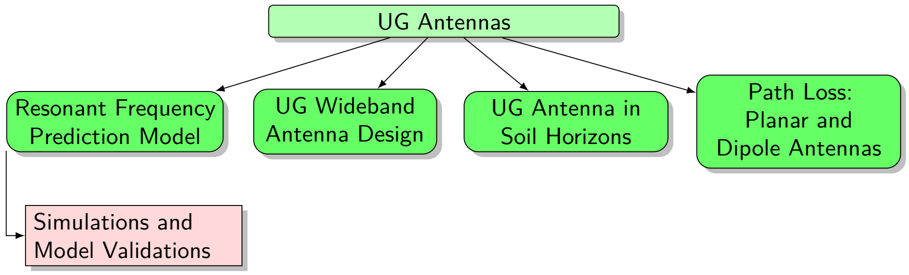

Fig. 6.1: Organization of the Chapter

soil types (silty clay loam, sandy, and silt loam soil) and indoor testbed. Fig. 6.1 shows the organizational structure of the chapter. The purpose of the model is to predict UG antenna resonance for designing efficient communication system for IOUT. Based on the model a wideband planar antenna is designed considering soil dispersion and soil-air interface reflection e ect which improves the communication range five times from the antennas designed only for the wavelength change in soil [54, 72].

IOUT is being used for implementing many applications [1, 12, 37, 52, 62, 74, 145]. In all these applications, major challenge is to establish a reliable communication. To that end, an underground-specific antenna design challenge is necessary to address. Three major factors that can impact the performance of a buried antenna are: 1) e ect of high soil permittivity changes the wavelength of EM waves, 2) variations in soil moisture with time a ecting the permittivity of the soil, and 3) di erence in how EM waves propagate during above-ground (AG) and underground (UG) communications.

For the third challenge above, it to be noted that lateral waves [20] are dominant component in EM [10], [40, 145], [139] during UG2UG communication and su ers lowest attenuation as compared to other, direct and reflected, components. Therefore, antennas used for over-the-air (OTA) communication will not be suitable for UG communication because of impedance mismatch. The chapter also focuses on developing an impedance model to study the e ect of changing wavelength in underground communication. Furthermore, it is discussed how soil-air interface and soil properties e ect the return loss of dipole antenna.

The use of antenna, in IOUT, di ers form traditional communication in that it is buried in the soil. There has been lot of work being done to study electromagnetic wave propagation in subsurface stratified media [6], [7], [8], [13], [20], [28, 42], [70], [72], [78], [79] . These studies uses fields of horizontal infinitesimal dipole of unit electric moment whereas, in practical applications, a finite size antenna is required. This section briefly sheds the light on work already done in the field.

In [28], authors calculates the depth attenuation and ground wave attenuation factor using two vector potentials for UG dipole without considering the impact of soil-air interface on current reflection. Currently, soil permittivity is calculated using soil dielectric model [26, 44, 54] which gives actual wavelength at a given frequency for elliptical planar antenna design in [41, 74]. The size of antenna in

[74] is determined by wavelength comparison using the same frequency in air and soil. However, it does not provide the required impedance match. In [32, 43, 80], authors performed experiments for Impulse Radio Ultra-Wide Band (IR-UWB) IOUT without considering the impact of soil-air interface. In [11], circularly polarized patch antenna is analyzed without considering the interface e ect. In another study [24, 33], communication between buried antennas are analyzed, however, the impact of orientation is not considered. Similarly, [18, 43] analyzes the performance of four buried antennas in refractory concrete without considering the concrete-air e ect.

To the best of our knowledge, there is no study which consider the impact of soil properties while designing the underground antennas. Therefore, rest of the discussion in this chapter is focused on developing a resonant frequency model which is capable of predicting the resonance at di erent soil moisture levels, soil types and depths. This information is useful in determining the transmission loss that may occur due to antenna mismatch in IOUT communications.The main focus of the model is to predict resonance, hence, impedance matching is ignored.

6.2 Resonant Frequency Prediction Model

6.2.1 Terminal Impedance and Soil Properties

Antenna Impedance Z_a is defined as a ratio of voltage and current at the input terminal of antenna. Complex power that is being radiated from the antenna can be calculated as by integrating Poynting's vector as given in [19, 40] as:

$$Z_a = \frac{1}{I^2} \int \int E \times H.da, \tag{6.1}$$

where I denotes the antenna current, da is perpendicular in the direction of surface of antenna, and $E \times H$ is energy per unit time. It can be assumed for perfectly conducting antenna that $\mathbf{E}(x,y,z) \equiv 0$, then impedance can be calculated as by integrating surface current density J_{se} and tangential electric field, and equation 6.1 becomes [19]:

$$Z_a = \frac{1}{I^2} \int \int E \times J_{se}.da, \tag{6.2}$$

By using the induced EMF method [12], equation (6.2) can be rewritten as:

$$Z_a = -\frac{1}{I(0)^2} \int_{-l}^{l} \mathbf{E_z}\, \mathbf{I}(\imath)\, d\zeta\ , \tag{6.3}$$

The electric field $\mathbf{E_z}$ is used for calculating the self-impedance of UG dipole antenna. $\mathbf{E_z}$ is produced by an assumed current distribution $\mathbf{I(0)}$ and current and electric field is integrated over the antenna surface. Homogeneous soil is considered for the measuring impedance and return loss of the antenna. For a buried dipole antenna, current appears in simple sinusoidal waveform given as:

$$I_0(\zeta) = I_m \sin[k_s(l - |\zeta|)] \,, \tag{6.4}$$

where I_m is the current amplitude, k_s represent complex wave number of the soil, l is the half length of the antenna, and $k_s = \beta_s + i\alpha_s = \omega\sqrt{\mu_0 \hat{\epsilon}_s}$ is the wave number in soil. $\mathbf{E_z}$ is given as:

$$\mathbf{E_z} = -\int_{-l}^{l} \frac{1}{4\pi j\omega\epsilon_s} \frac{e^{-jk_s r}}{R} \left(\frac{\partial^2}{\partial\zeta^2} + k_s^2\right) I(\zeta) d\zeta, \tag{6.5}$$

By substituting the $\mathbf{E_z}$ in equation (6.5) and $\mathbf{I(0)}$ from equation (6.4) in equation (6.2) we get [23, 44]:

$$Z_a \approx f_1(\beta l) - i\left(120\left(\ln\frac{2l}{d} - 1\right)\cot(\beta l) - f_2(\beta l)\right) \,, \tag{6.6}$$

where

$$f_1(\beta_s l) = -0.4787 + 7.3246\beta_s l + 0.3963(\beta_s l)^2 + 15.6131(\beta_s l)^3 \tag{6.7}$$

$$f_2(\beta_s l) = -0.4456 + 17.0082\beta_s l - 8.6793(\beta_s l)^2 + 9.6031(\beta_s l)^3 \tag{6.8}$$

β_s is the real part of the wave number k_s, d is the diameter of the dipole, and l is half of the length of the dipole. βl is expressed as

$$\beta_s l = \frac{2\pi l}{\lambda_0} \mathrm{Re}\left\{\sqrt{\epsilon_s}\right\} \,, \tag{6.9}$$

where ϵ_s is the relative permittivity of soil and λ_0 is the wavelength in air. Since the ϵ_s is dependent on frequency, βl is not a linear function of l/λ_0. Therefore, when the medium is changed from soil to air, both, resonant frequency and impedance at the resonant frequency of the antenna, also changes.

Practical IOUT has motes deployed at 0.3m - 1m [37, 61] and there is high impact of soil -air interface at these depths, hence, environment cannot be modeled. Next, the environment is modeled to study the impact on antenna return loss and impedance due to reflection of waves by soil-air interface. Upon excitement of antenna, a current distribution of $I_0(\zeta)$ is generated and propagated wave is either reflected or refracted form soil-air interface. E_r and I_r are the reflected electric field and induced current, respectively that reaches the antenna.

I_r and Z_r, resulting impedance are modeled due to field generated from imaginary dipole in homogeneous soil. As current distribution (6.4), E_r field reflected due to the soil-air interface at the antenna is [12, 38]:

$$E_r = -i30I_m\left(\frac{e^{-ik_s r_1}}{r_1} + \frac{e^{-ik_s r_2}}{r_2} - 2\cos k_s l \frac{e^{-ik_s r}}{r}\right) \times \Gamma \,, \tag{6.10}$$

where

$$r = [(2h)^2 + \zeta^2]^{1/2} \,, \tag{6.11}$$

$$r_1 = [(2h)^2 + (\zeta - l)^2]^{1/2} \,, \tag{6.12}$$

$$r_2 = [(2h)^2 + (\zeta + l)^2]^{1/2} \,, \tag{6.13}$$

h represents the burial depth of the antenna, and reflection coefficient at the soil-air interface Γ is measured as:

$$\Gamma = \frac{2}{1 + k_0/k_s} - 1 = \frac{2}{1 + \sqrt{\frac{1}{\epsilon_s}}} - 1 \,, \tag{6.14}$$

and k_0 is the wave number in air.

The antenna impedance is given as: $Z_a^u = Z_a . \frac{I_0}{I_r^2}$ and from this impedance values the return loss of the antenna is given as:

$$RL_{dB} = 20\log_{10}\left|\frac{Z_s + Z_a^u}{Z_s - Z_a^u}\right| . \tag{6.15}$$

The reflection coefficient Γ is given as: $|\Gamma| = 10^{\frac{RL}{20}}$. Reflection coefficient is transformed to impedance by using: $Z_a^u = Z_s \frac{1+\Gamma}{1-\Gamma}$. Standing wave ratio (SWR) is expressed as: $SWR = \frac{1+|\Gamma|}{1-|\Gamma|}$

6.2.2 Defining Resonant Frequency

The frequency where the antenna's input impedance is pure resistance is known as resonant frequency f_r. i.e.,

$$Z_a^u|_{f=f_r} = Z_r = R_a. \tag{6.16}$$

and where return loss is maximum such that:

$$f_r = \max(RL_{dB}). \tag{6.17}$$

A comparative performance analysis is done between this analytical model with resonant frequency of permittivity-based antenna by using: $f_r = f_0/\sqrt{\epsilon_s}$, where f_0 represents an OTA resonant frequency, and ϵ_s is the permittivity of the soil.

6.2.3 Bandwidth Expression

It is very difficult to find a closed-form bandwidth formula for the UG antenna because of involvement of many soil and antenna factors, however, a resonant frequency-based bandwidth expression (BW) can be calculated as [62]:

$$BW = \begin{cases} 0 & \text{if -}RL_{dB}(f) > \delta, \\ 2(f - f_m) & \text{if -}RL_{dB}(f) \leq \delta \text{ and } f < f_r, \\ 2(f_M - f) & \text{if -}RL_{dB}(f) \leq \delta \text{ and } f \geq f_r, \end{cases} \tag{6.18}$$

where f_r is the resonant frequency, f_m and f_M are the lowest and highest frequency at which $RL_{dB}(f) \leq \delta$. There is no fixed value of δ, however, value of $10\,\mathrm{dB}$ is generally used in the literature [9].

6.3 Simulations and Experiment Setup

Following simulation setup was used to analyze the performance of underground dipole antenna: CST Microwave Studio Suite (MWS) [1], an indoor testbed without changing the soil parameters. Simulations are conducted with antenna buried 20cm inside the soil, and distances of 5cm-12m from the first antenna. The results from this testbed was compared with outdoor testbed with dipole antenna in silty clay loam soil. Vector Network Analyzer (VNA) is used for measuring antenna S_{11} and channel responses to frequency.

6.4 Model Validations

6.4.1 Model, Simulation, and Empirical Results

Figs. 6.2(b), 6.2(a) and 6.2(c) compares theoretical, measure and simulated return loss at 20cm of depth in silt loam, sandy and silt clay soil type, respectively. It can seen that all three results (measured, theoretical and simulated) confirm each other with minor di erences. For example, at resonant frequency, for silt loam soil, the measured and model return loss matches whereas simulated return loss di ers by 7% and this di erence drops to 1% for sandy soil. This 1% - 7% di erence is because of the uncertainties soil simulation software.

Figs. 6.3 compares the resonant frequency and bandwidth from measured experiment and theoretical model for 20% VWC. The results are for sandy (Figs. 6.3(a) and 6.3(b)) and silt loam soil (Figs. 6.3(c) and 6.3(d)) at varying depths ranging from 10cm - 40cm. For sandy soil, both, measured resonant frequency and bandwidth, matches the model value with minor di erence of 0.01% - 1.93% in

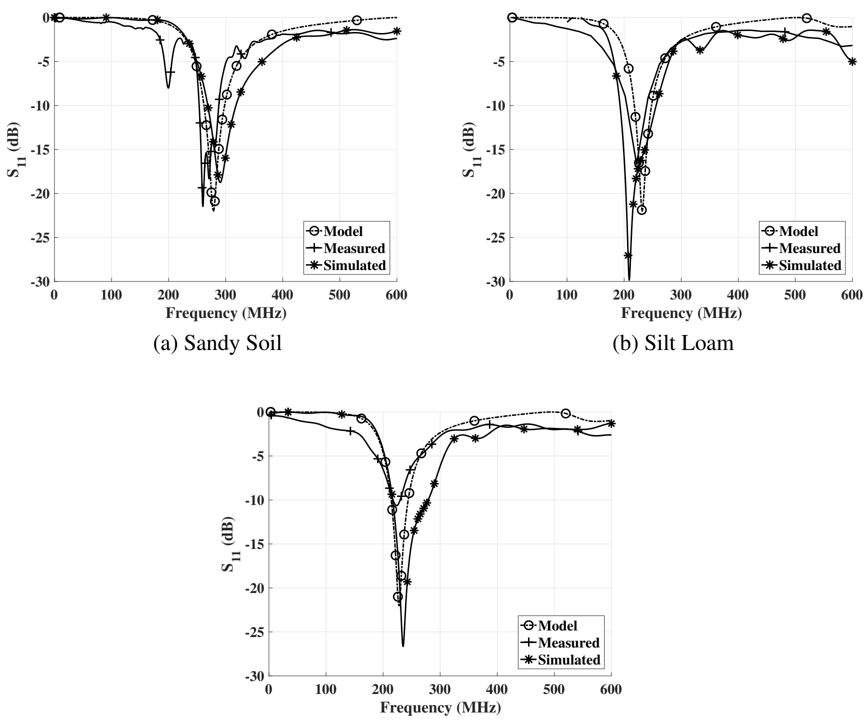

(a) Sandy Soil

(b) Silt Loam

(c) Silty Clay Loam

Fig. 6.2: Comparative analysis of return loss estimated from simulated, theoretical, measured experiments in [66]: Sandy soil b) Silt Loam soil c) Silty clay loam soil

resonant frequency and 2.77 MHz - 4 MHz in bandwidth. For silt loam soil, both, measured resonant frequency and bandwidth, matching trend between both models is same with minor di erence of 1.01% - 3.53% in resonant frequency and 1 MHz - 8 MHz in bandwidth. These di erences between the models is because of change in return loss and resonant frequency at some particular depth which leads to di erence in bandwidth. However, these variations do not e ect the UG communication as antenna bandwidth is higher than these variations [39, 65, 139].

Other reasons for di erences in model could be: 1) abrupt phase changes of waves while transition from one depth to other and due to soil-air interface impact, and 2) theoretical model do not consider the EM waves propagation e ect in coaxial cable connected to antenna. Overall the resonant frequency matched with the model matched each other and comparing measurements with theoretical model makes it a powerful tool to analyze the underground antenna.

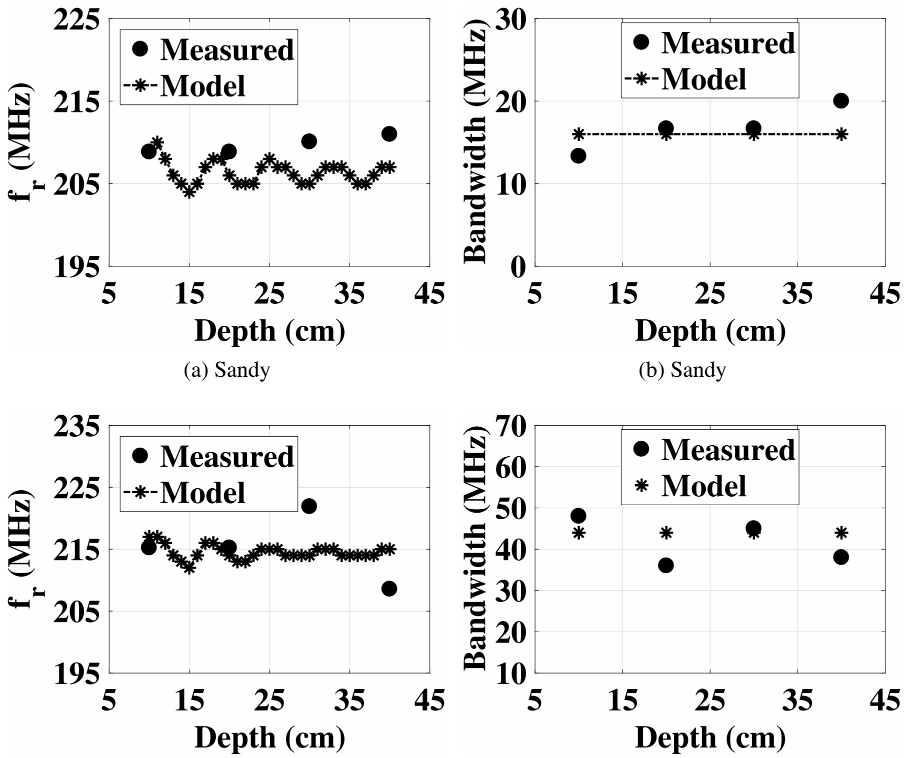

(a) Sandy (b) Sandy

(c) Silt Loam (d) Silt Loam

Fig. 6.3: Comparative analysis of theoretical and measured experiments at di erent depths for [66]: a) Resonant frequency (sandy), b) Bandwidth (sandy), c) Resonant frequency (silt loam), and d) Bandwidth (silt loam soil)

6.4.2 Analysis of Impact of Operation Frequency

Figs. 6.5 plots the resonant frequency and return loss for 5% - 40% soil moisture level. The results are for sandy (Figs. 6.5(a) and 6.5(b)) and silt loam soil (Figs. 6.5(c) and 6.5(d)). Resonant frequency decreases 62% (from 369 MHz to 137 MHz) for silt loam soil, and decreases 59% (from 357 MHz to 146 MHz) for sandy soil [25, 27].

Resonant frequency, of a dipole antenna, in soil and OTA is represented by f_{rs} and f_{ro}, respectively. Figs. 6.4 compares the ratio $\frac{f_{rs}}{f_{ro}}$ and antenna permittivity 433MHz and 915MHz. The results are for sandy (Figs. 6.4(b) and 6.4(d)) and silt loam soil (Figs. 6.4(a) and 6.4(c)) at varying depths ranging from 10cm - 40cm. At di erent depths, change in resonant frequency di erence is di erent , and ratio is also varying as compared to the OTA [35].

The di erence is clear in figs. 6.6 where di erence in resonant frequency δ of theoretical model and antenna based on soil permittivity only, δ, is shown with

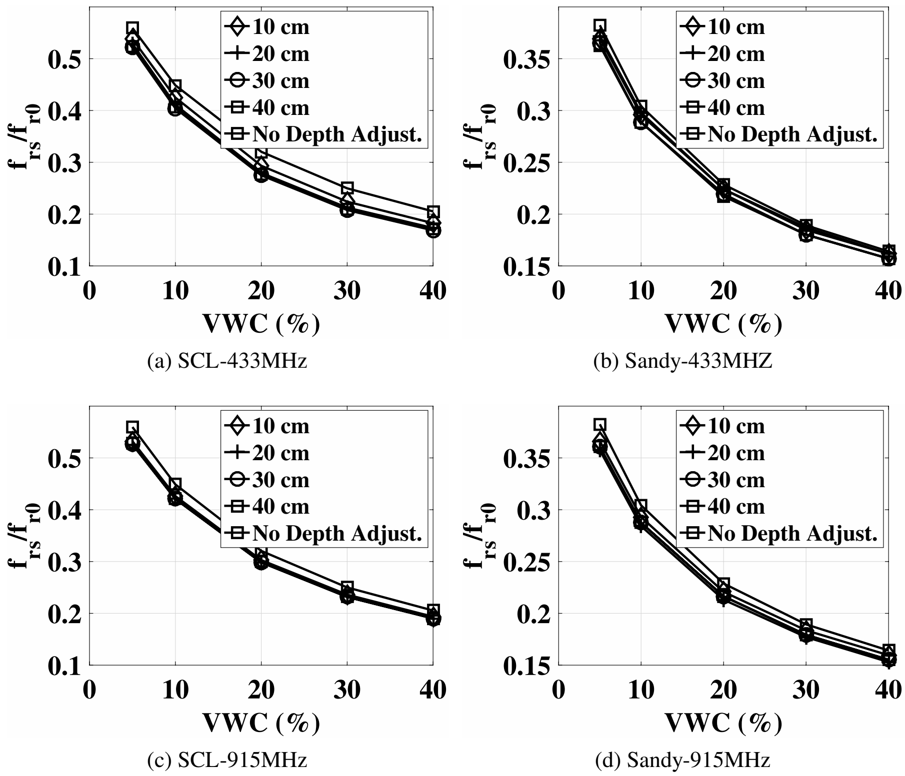

Fig. 6.4: E ect of VWC on ratio of resonant frequency in soil and OTA in [66]: (a) Silty Clay Loam Soil at 433 MHz, (b) Sandy soil at 433 MHz, (c) Silty Clay Loam Soil at 915 MHz, and (d) Sandy Soil at 915 MHz

varying soil moisture levels at 433MHz and 915MHz. The results are for sandy (Figs. 6.6(b) and 6.6(d)) and silt loam soil (Figs. 6.6(a) and 6.6(c)) at varying depths ranging from 10cm - 40cm. It can be seen that δ is inversely proportional to soil moisture level. For example, δ increase by 10 Mhz - 15 MHz when frequency goes from 433 MHz - 915 MHz which proves that only permittivity-based IOUT system su ers performance degradation and highlights the importance of considering impact of soil-air interface. Hence, consideration of burial depth is important for efficient IOUT communication system [34, 43].

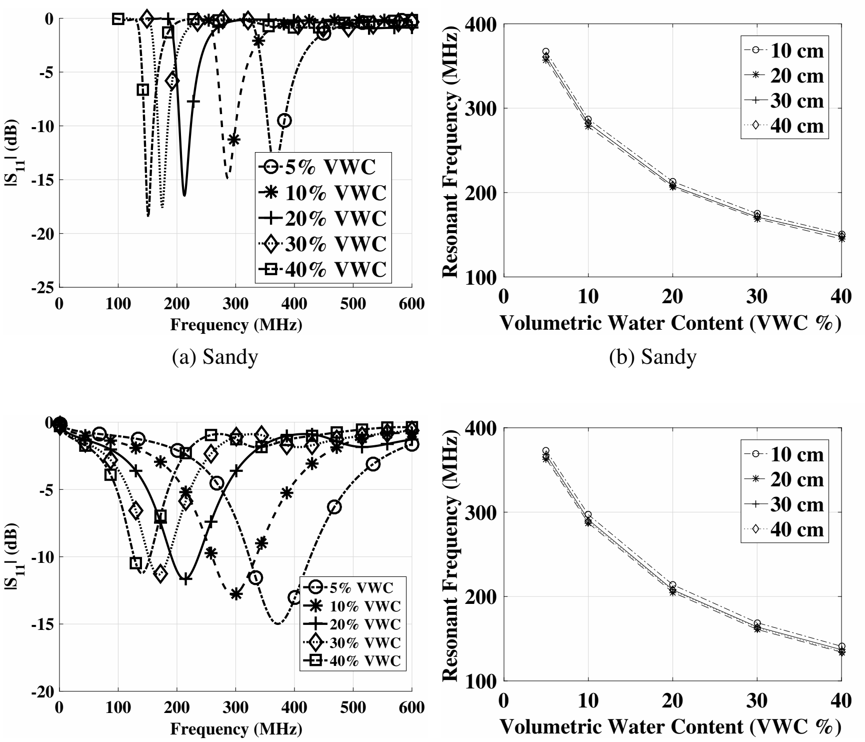

(a) Sandy (b) Sandy

(c) Silt Loam (d) Silt Loam

Fig. 6.5: Theoretical Results [66]: (a) Return Loss in Sandy Soil, (b) Resonant Frequency in Sandy soil, (c) Return Loss in Silt Loam Soil, and (d) Resonant Frequency in Silt Loam Soil

6.5 Underground Wideband Antenna Design

To compensate for the shift of resonant frequency of UG dipole antenna, a wideband antennas of di erent sizes and 433MHz frequency are designed and fabricated for testing.

1. ***Radiation Pattern in UG Communications:*** The radiation pattern of the antenna is an added advantage for using this antenna. Out of three paths [20, 33] (direct wave, reflected wave and lateral wave) in UG communication, lateral wave is the most dominant in far-field [42, 61], [46, 67]. Therefore, radiation pattern must have maximum lateral wave component. [20], [36, 67] shows that lateral wave only occur when incident angle is at critical angle θ_c. θ_c changes with the varying soil moisture and is less than 15° in all soil moisture settings. The radiation pattern is unidirectional towards soil-air interface, thus, desirable radiation pattern can be achieved if antennas are placed parallel to soil-air interference.
2. ***The Return Loss:*** Figs. 6.8 and 6.9 shows the return loss and bandwidth at varying depths (0.13m, 0.3m, and 0.4m) for three di erent soil moisture values

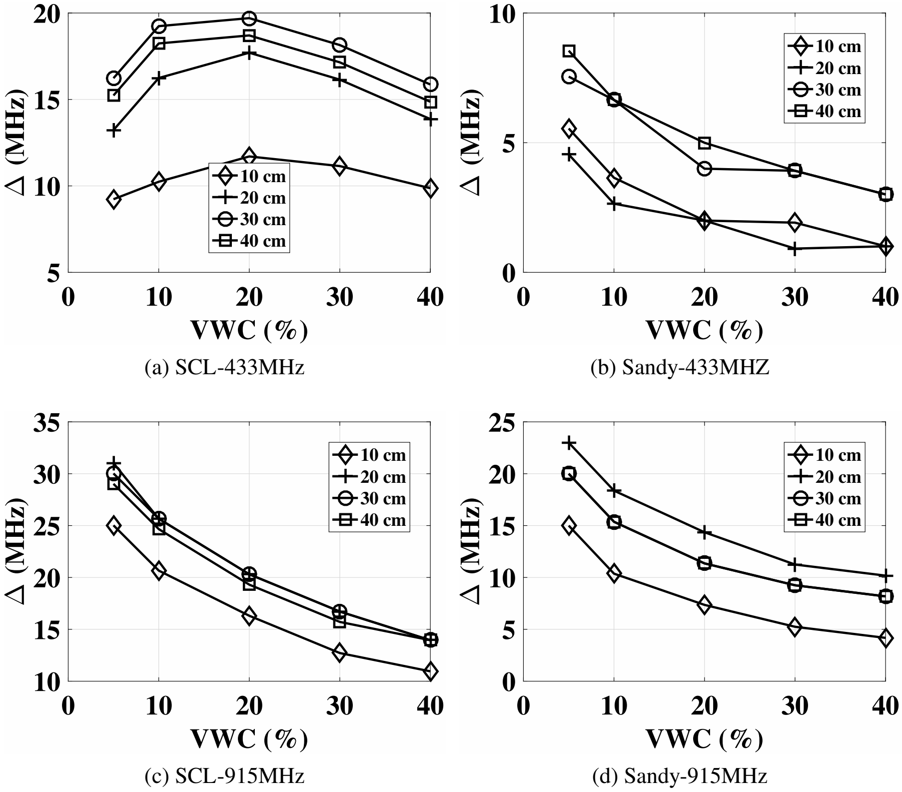

Fig. 6.6: Δ v/s VWC [66]: (a) Silty Clay Loam Soil at 433 MHz, (b) Sandy soil at 433 MHz, (c) Silty Clay Loam Soil at 915 MHz, and (d) Sandy Soil at 915 MHz

(10%, 30% and 40%). The resonant frequency varies in all these scenarios, however, return loss remains below 10dB for all depths and moisture levels [28].

3. ***Communication Results:*** The designed planar antenna is compared with 25mm wideband antenna and elliptical antenna in testbed to evaluate the performance for underground-aboveground communications. Two motes are used for UG and AG with planar and Yagi antenna, respectively to accomplish UG2AG and AG2UG channel communication [30]. Fig. 6.10 plots the received signal strength (RSS) with changing distance. It shows that although the communication range of 200m is achieved but practical multi-hop connectivity is still limited in underground communication. For UG2AG channel, the designed antenna increases the communication range by 587.5% as compared to elliptical antenna (from 8m to 55m) and 223.5% as compared to circular antenna (from 17m to 55m). For UG2AG channel, the designed antenna increases the communication range by 587.5% as compared to elliptical antenna (from 8m to 55m) and 266.7%

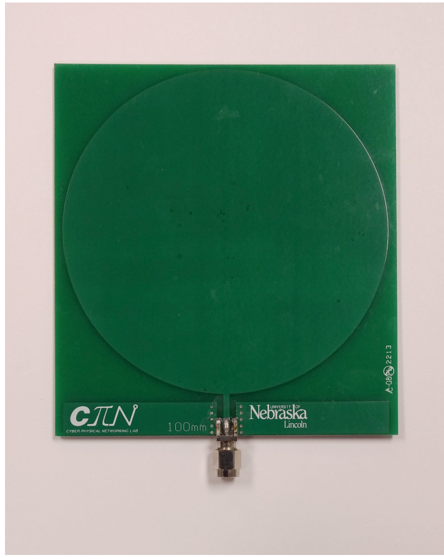

Fig. 6.7: UG wideband planar antenna [66]

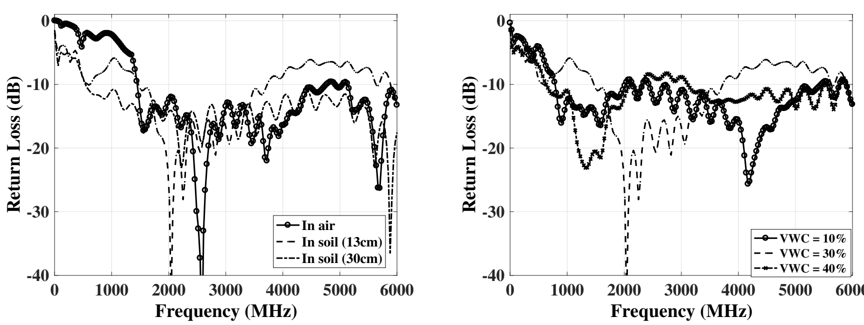

(a) (b)

Fig. 6.8: Return loss using wideband planar antenna[66]: (a) Depths, and (b) Volumetric water content

as compared to circular antenna (from 15m to 55m) [29]. These results shows that designing an antenna specific for UG environment is critical for IOUT system.

6.6 Underground Antenna in Soil Horizons

Precision agriculture is the practice of accurately capturing the changing parameters of the soil including water infiltration and retention, nutrients supply, acidity, and

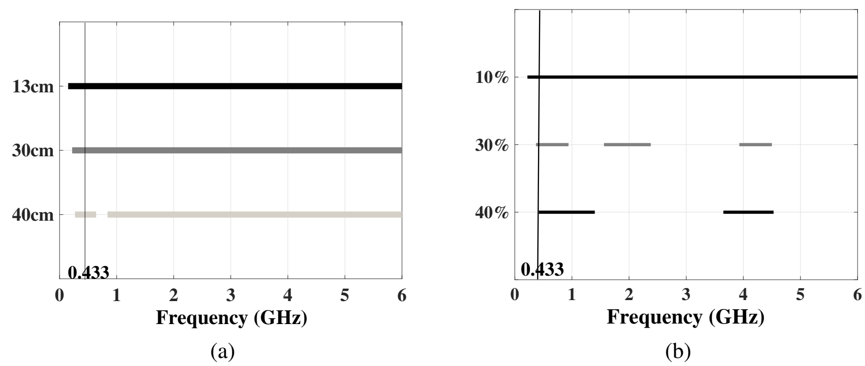

Fig. 6.9: Bandwidth of wideband planar antenna (100mm) at (a) varying Depths and (b) varying soil moisture [66]

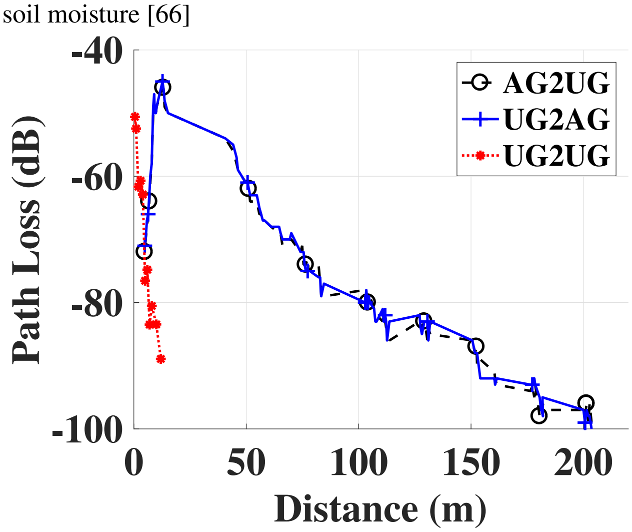

Fig. 6.10: Path loss with varying distance for different communication links [66]

other time changing phenomena by using the modern technologies. Using precision agriculture, fields can be irrigated more efficiently hence conserving water resources and increasing productivity. Wireless underground sensor networks (WUSN) are being used to monitor the soil for smart irrigation. Communication in wireless underground sensor networks is affected by soil characteristics such as soil texture, volumetric water content (VWC) and bulk density. These soil characteristics vary with soil type and soil horizons within the soil. In this section we have investigated the effects of these characteristics by considering Holdrege soil series and homogeneous soil. It is shown that consideration of soil characteristics of different soil horizons leads to (5-6 dB) improved communication in wireless underground sensor networks [26, 53].

Horizons are layers of soil which are formed by four soil processes and have unique chemical, physical, and visible characteristics. These soil process are additions, losses, transformations, and translocation. There are five horizons: O, A, E, B, and C. In soil, these horizons can form in any order. Some soils do not contain all horizons and in some soils multiple horizons can repeat. Horizons A, B are of most interest because of their high impact on plant growth.

In wireless underground sensor networks sensor nodes are buried in soil. Establishment of wireless communication links is important for data communication. As each soil horizon have unique soil texture, bulk density and water holding capability. Also depth and width of each horizon di ers in di erent type of soils. These factors have a significant influence on the performance of a buried antenna and communication. In [51], impact of these soil factors on underground communication is analyzed and given as follow:

Soil Moisture
: Soil moisture changes with time due to climate and irrigation, which influence the soil permittivity.

Soil permittivity
: Electromagnetic waves propagation in soil exhibit di erent characteristics in soil due to higher permittivity of soil.

Soil-Air Interface
: Impedance of under ground antenna is changed because of current disturbance at antenna due to reflection from soil-air interface [30, 61, 74].

In this section, by using our model for underground to underground (UG2UG) communications [46], we have analyzed the performance of wireless underground channel by using Holdrege soil profile [3] and homogeneous soil. Moreover, we provide analytical results for path loss for three di erent scenarios including same soil moisture level across all horizons, water infiltration and water retention scenario.

Based on the analysis it is shown that that antennas buried into soil horizons by taking soil characteristics into account experience less path loss as compared to antenna buried in homogeneous soil and path loss is decreased from 5-6 dB. It is also shown that path loss varies with soil moisture and increase in soil moisture also increase the path loss for all type of soils. It is also evident that in underground wireless sensor networks path loss increase with frequency therefore low operation frequencies are suitable for for wireless underground communication.

To get a wavelength in soil at a given frequency, soil permittivity is calculated using the dielectric model [26, 49, 52, 54]. This wavelength calculated by the dielectric gives insight into design of antenna [30, 74]. For underground communications antenna are buried in di erent depths in soil. Theoretical analysis EM field of antennas in infinite dissipative medium is presented in [19, 24, 32, 55]. Return loss of the antenna is not considered in this analysis. Measurements of dipole antennain solution are presented in [22]. Because of the di erence in permittivity of soil and permittivity solution this work in not applicable to wireless underground sensor

Fig. 6.11: Holdredge Soil Profile

Table 6.1: Holdrege Soil - physical characteristics

Horizon	Depth in inches	Sand	Slit	Clay	Textual Class
Ap	0-7	16.6	61.4	22.0	Silt Loam
A	7-13	12.0	58.4	29.6	Silt Clay Loam
Bt1	13-16	13.3	55.3	31.4	Silt Clay Loam
Bt2	16-24	11.2	58.9	29.9	Silt Clay Loam

networks. Current disturbance at antenna due to reflection from soil-air interface is mentioned in [21] but its impact are not analyzed. In [54] we have analyzed these impacts on underground antenna using homogeneous soil. We have also developed a three wave channel model for wireless underground communications in [9, 27, 61].

6.6.1 Holdrege Soil Characteristics

We have used Holdrege soil and homogeneous soil for our analysis. Table 6.1 shows physical properties Holdrege soil.

We have selected Holdrege series because it is one of the well-drained, highly productive and most fertile soil in the Nebraska, United States. It is also official state

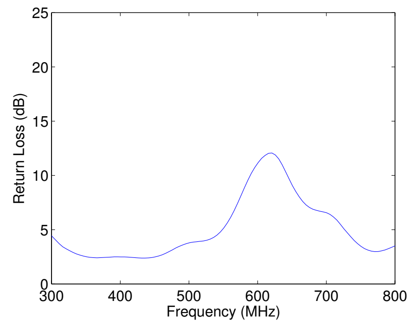

Fig. 6.12: Return Loss of the Antenna

soil of Nebraska and almost all the soil is under cultivation. As per United States Department of Agriculture [3]:

Prairie environment has contributed to formation of horizontal layers in profile of Holdrege series. Clay and lime particles have moved downward in profile due to drainage of water inside the profile. Due to interaction of these processes there is thick, dark color topsoil, a clay enriched subsoil and a substratum containing free lime. Holderede soil is very well irrigated and is a extensively cultivated soil. Corn and soy are the main crops.

6.6.2 Numerical Analysis

We have considered three cases for analytical evaluation. First case we have compared the two soils under the same soil moisture case for all soil horizons and depths. In second case we analyses the the water infiltration scenario in which top soil horizons have more water content than the subsoil horizons. Third case compares the water retention scenario in which subsoil is more saturated as compared to the topsoil. We have used frequency range of 300 MHz to 800. Transmitted power is 15 dBm. Return Loss of the antenna used in the evaluation is shown in Figure . Antennas are buried at four depths. Four antenna burial depth corresponds to four di erent horizons (Ap, A, Bt1, Bt2)of Holdrege soil as shown in Table 1. For homogeneous soil these are 10 Cm, 20 Cm, 30 Cm and 40 Cm. Horizontal distance distance between transmitter receiver is 50 Cm. Bulk density is 1.5 grams/cm3 and particle density is 2.66 grams/cm3.

6.6.3 Same Soil Moisture Scenario

Fig. 6.13 shows the path loss for two soil types for Volumetric Water Content (VWC) of value of 10%. For all depths and across all frequency range Path loss for homogeneous soil is 5 dB to 6 dB higher than as compared to Holdrege soil.

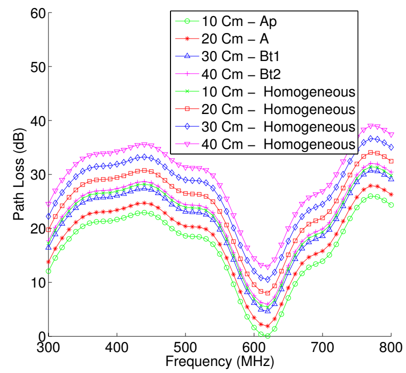

Fig. 6.13: Path Loss vs. Frequency - VWC 10%

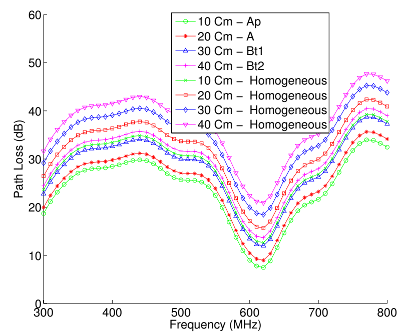

Fig. 6.14: Path Loss vs. Frequency - VWC 20%

Moreover between 550 MHz to 650 MHz range path loss is low because of the low return loss of the antenna. It is also clear that path loss increases with frequency.

Fig. 6.14 shows the path loss for two soil types for Volumetric Water Content (VWC) of value of 20%. For all depths and across all frequency range Path loss for homogeneous soil is 5 dB to 6 dB higher than as compared to Holdrege soil. Due to 10% increase in water content there is an increase of 8 dB for all horizons.

Fig. 6.15 and Fig. 6.16 shows the path loss for two soil types for Volumetric Water Content (VWC) of value of 30% and 40%. For both soil moisture levels, for all depths and across all frequency range path loss for homogeneous soil is 5 dB to 6 dB increased as compared to Holdrege soil. Path loss for 30% and 40% is considerably higher than dry than the 10%.

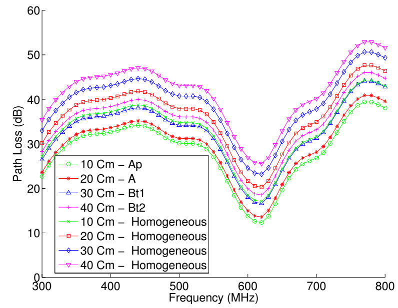

Fig. 6.15: Path Loss vs. Frequency - VWC 30%

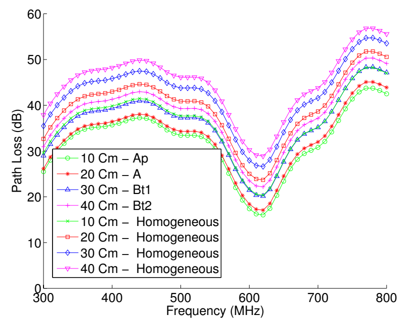

Fig. 6.16: Path Loss vs. Frequency - VWC 40%

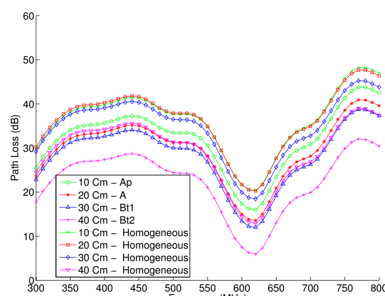

Fig. 6.17: Path Loss vs. Frequency - Water Infiltration Scenario%

6.6.4 Water Infiltration Scenario

In this case we consider the scenario in which higher horizons have more water content as compared to lower soil horizons. Fig. 6.17 shows the path loss when Ap horizon have 40% VWC, A horizon have 30% VWC, Bt1 have 20% VWC and Bt2 have 10% VWC. It is evident that communication performance is best at Bt2 horizon because of low water content.

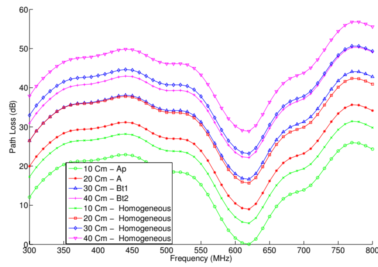

Fig. 6.18: Path Loss vs. Frequency - Drainage Scenario%

6.6.5 Water Retention Scenario

In this case we consider the scenario in which lower horizons have more water content as compared to higher soil horizons. Fig. 6.18 shows the path loss when Ap horizon have 10% VWC, A horizon have 20% VWC, Bt1 have 30% VWC and Bt2 have 40% VWC. Antenna buried at the A horizon experience lower path loss because of low attenuation due to lower VWC.

In this section, the impacts of soil texture, soil moisture on burial depth of antenna in di erent soil horizons and on path loss are analyzed for underground wireless communications in Holdrege soil and homogeneous soil. It is shown that antennas buried into soil horizons by taking soil characteristics into account experience less path loss as compared to antenna berried in homogeneous soil. It is also shown that path loss varies with soil moisture and increase in soil moisture also increase the path loss for all type of soils. It is also evident that in underground wireless sensor networks path loss increase with frequency therefore low operation frequencies are suitable for for wireless underground communication.

6.7 Path Loss Variations with Planar and Dipole Antennas

The digital agriculture [38, 48, 62, 68, 75] is the area in which technology is used to e ectively manage agriculture by understanding the temporal and spatial changes in soil, crop, production, and management through innovative techniques. The analysis of the communication path loss is vital for an efficient communication system design in sensor-guided irrigation management system. To investigate propagation loss variations, the path loss experiments are conducted in sandy soil testbed, and greenhouse outdoor silty clay loam testbed using a wideband planar antenna [50, 54] and dipole antennas.

6.7.1 Experiment Setup

In a sandy soil testbed [54, 61], two planar antennas, are buried at $20cm$ depth at a distance of $1m$. The return loss and path loss measurements are taken. To analyze the e ects of a planar in the middle of two planar, obstructing the communications, another planar antenna is buried in the middle at $50cm$ distance and same depth ($20cm$). Accordingly, the path loss and return loss measurements are taken again for $50cm$ distance and $1m$ distance [20, 48].

In the greenhouse, another testbed of planar antennas is commissioned in silty clay loam soil. To compare the results of the experiment with sandy soil testbed, same empirical parameters are used. First, the path loss and return loss measurements are taken for planar buried at $1m$ distance at $20cm$ depth. Afterward, another planar is installed at $50cm$ distance and $20cm$ depth, and return loss and path loss measurements are taken, again, first for $1m$ distance and then for $50cm$ distance [72, 76].

To compare the results of planar antennas with dipole antenna, a testbed of dipole antennas is developed outside of the greenhouse in silty clay loam soil. In this testbed, three dipole antennas are buried in soil at $50cm$ distance each and burial depth is $20cm$. The physical properties of sandy soil and silty clay loam soil are shown in Table 7.3. The results of this empirical campaign are presented in Section 7.4. The return loss of dipole and planar antennas are shown in Fig. 6.19. The comparison of dipole and planar return loss in same soil is given in Fig. 6.20.

Table 6.2: Soil used in testbeds - physical characteristics

Textural Class	**S**and %	**S**ilt %	**C**lay %
Silty Clay Loam	13	55	32
Sandy Soil	86	11	3
Silt Loam	33	51	16

6.7.2 Results

The planar antenna path loss at $50cm$ and $100cm$ in sandy soil and silty clay loam testbed is shown in Fig. 6.21(a) and Fig. 6.21(b), respectively. In sandy soil, there is 14dB di erence in path loss when communication distance is increased from $50cm$ to $100cm$. Similarly, in silty clay loam soil, at frequencies higher than 500MHz path loss is increased from 19dB [25, 46].

In Fig. 6.20(c), the path loss comparison of dipole and planar antenna is shown in sandy soil testbed at $50cm$. The variations in path loss with change in frequency, present in the case of dipole antenna, are not observed when measurements are taken using planar antenna. Similarly in Fig. 6.20(d), the path loss comparison of dipole

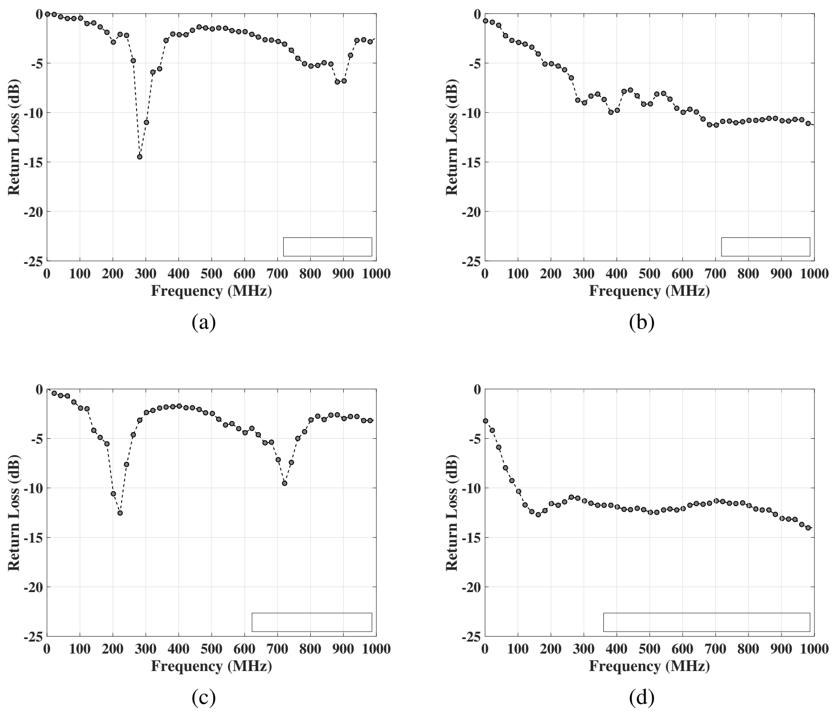

Fig. 6.19: Return loss: (a) sandy soil with dipole antenna, (b) sandy soil with planar antenna, (c) silty clay with dipole antenna, (d) silty clay with loam planar antenna

and planar antenna is shown in silty clay loam testbed at $50cm$. As observed in sandy soil, the variations in path loss with frequency present in dipole antenna are not observed when using planar antenna [46, 47].

The change in path loss when a planar is buried between planar antennas is shown in Fig. 6.22(a) for sandy soil and in Fig. 6.22(b) for silty clay loam. In sandy soil, di erence of 8dB is observed at frequencies less than 400MHz, and in silty clay loam overall there is di erence except 4-5 dB di erence at 300 MHz and 800 MHz [29, 33].

The path loss di erence using same antenna at $50cm$ and $100cm$ distance in di erent soils is presented in Fig. 6.22(c) and Fig. 6.22(d), respectively. A 28dB lower path loss is observed in sandy soil when compared to silty clay loam both at 50cm and 100cm distance. This happens because the sandy soil holds less bounded water which is the major component in soil that absorbs electromagnetic waves [29]. A propagation path loss analysis has been presented using dipole and planar antennas in the sandy and silty clay loam. In the sandy soil, better radio wave propagation is observed. The results show that the planar antenna is more efficient for subsurface communications. The analysis is useful to determined inter-node distance in sensor-guided irrigation system.

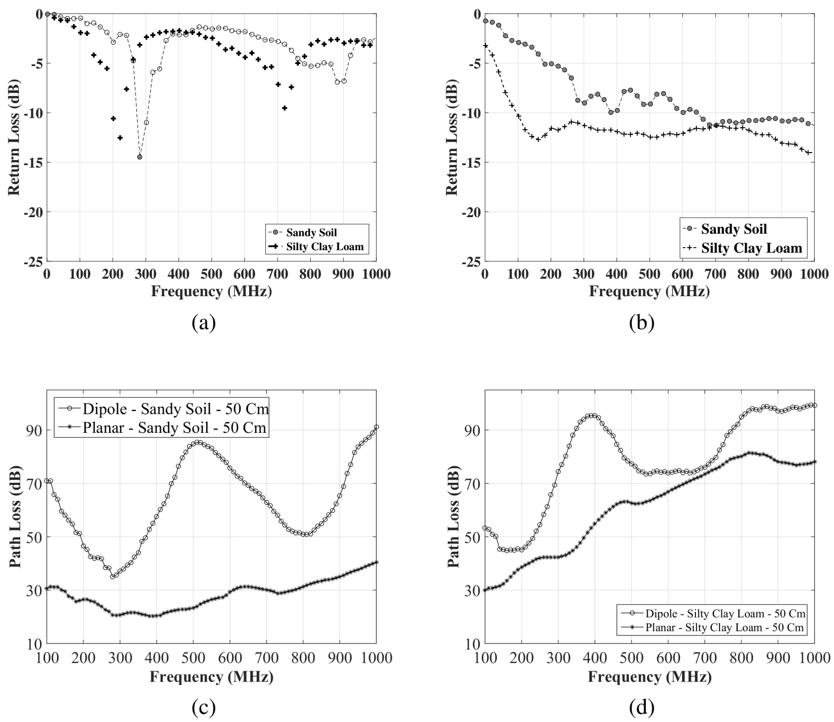

Fig. 6.20: Return Loss Comparison: (a) Dipole antennas only, (b) Planar antennas only, (c) using Dipole and Planar Antenna in sandy soil, (d) using Dipole and Planar Antenna in in Silty Clay Loam Soil

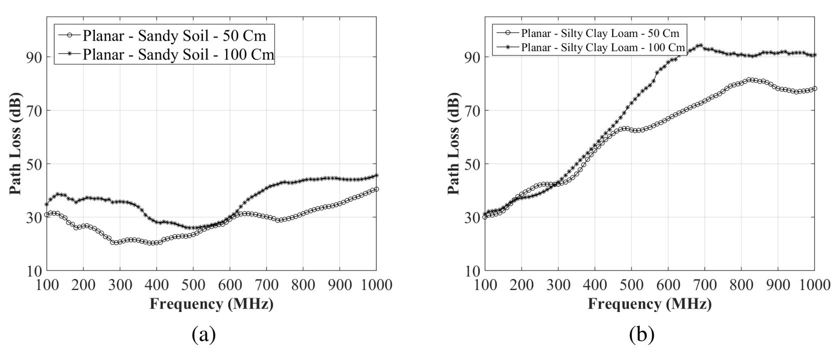

Fig. 6.21: Path Loss comparison: (a) Planar antenna in sandy soil, (b) Planar antenna in silty clay loam,

References

[1] (2020) CST Microwave Studio. `www.cst.com/products/cstmws`

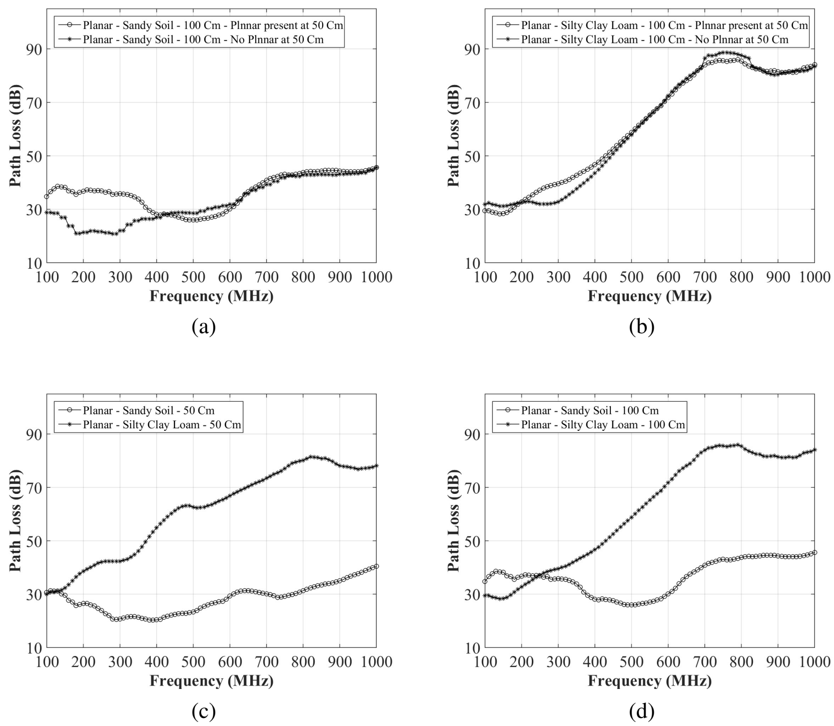

Fig. 6.22: (a) Planar antenna in sandy soil, (b) Planar antenna in silty clay loam, (c) Dipole and planar antenna in sandy soil, (d) Dipole and planar antenna in silty clay loam soil

Fig. 6.23: Path Loss comparison: (a) Planar antenna placed between two planar antenna (sandy), (b) Planar antenna placed between two planar antenna (silty clay loam), (c) Planar antenna in both soil place at a distance of 50cm, (d) Planar antenna in both soil place at a distance of 100cm,

[1] Abrudan TE, Kypris O, Trigoni N, Markham A (2016) Impact of rocks and minerals on underground magneto-inductive communication and localization. IEEE Access 4:3999–4010, DOI 10.1109/ACCESS.2016.2597641

[3] of Agriculture UD (2014) Census of Agriculture. URL `http://www.agcensus.usda.gov/`

[52] Akyildiz IF, Stuntebeck EP (2006) Wireless underground sensor networks: Research challenges. Ad Hoc Networks Journal

[54] Akyildiz IF, Sun Z, Vuran MC (2009) Signal propagation techniques for wireless underground communication networks. Physical Communication Journal (Elsevier) 2(3):167–183

[6] Arnautovski-Toseva V, Grcev L (2016) On the image model of a buried horizontal wire. IEEE Transactions on Electromagnetic Compatibility 58(1):278–286

[7] Banos A (1966) Dipole radiation in the presence of a conducting halfspace. Pergamon Press
[8] Biggs A (1968) Dipole antenna radiation fields in stratified antarctic media. Antennas and Propagation, IEEE Transactions on 16(4):445–448, DOI 10.1109/TAP.1968.1139227
[9] Bird TS (2009) Definition and misuse of return loss [Report of the transactions Editor-in-Chief]. IEEE Antennas and Propagation Magazine 51(2):166–167, DOI 10.1109/MAP.2009.5162049
[10] Brekhovskikh LM (1980) Waves in Layered Media. Academic Press, New York
[11] Castorina G, Donato LD, Morabito AF, Isernia T, Sorbello G (2016) Analysis and design of a concrete embedded antenna for wireless monitoring applications. IEEE Antennas and Propagation Magazine 58(6):76–93
[12] Dong J, Shen F, Dong Y, Wang Y, Fu W, Li H, Ye D, Zhang B, Huangfu J, Qiao S, Sun Y, Li C, Ran L (2016) Noncontact measurement of complex permittivity of electrically small samples at microwave frequencies. IEEE Transactions on Microwave Theory and Techniques 64(9):2883–2893, DOI 10.1109/TMTT.2016.2588487
[13] Dong S, Yao A, Meng F (2015) Analysis of an underground horizontal electrically small wire antenna. Journal of Electrical and Computer Engineering 2851:9
[61] Dong X, Vuran MC (2011) A channel model for wireless underground sensor networks using lateral waves. In: Proc. of IEEE Globecom ’11, Houston, TX
[62] Dong X, Vuran MC (2013) Impacts of soil moisture on cognitive radio underground networks. In: Proc. IEEE BlackSeaCom, Georgia
[9] Dong X, Vuran MC, Irmak S (2012) Autonomous precision agricultrue through integration of wireless underground sensor networks with center pivot irrigation systems. Ad Hoc Networks (Elsevier)
[12] Elliott RS (1981) Antenna Theory and Design. Prentice-Hall, Inc.
[18] Fitzgerrell RG, Haidle LL (1972) Design and performance of four buried uhf antennas. IEEE Trans Antennas Propagation 20(1):56–62
[19] Galejs J (1969) Antennas in Inhomogeneous Media. Pergamon Press
[20] Hansen R (1963) Radiation and reception with buried and submerged antennas. IEEE Transactions on Antennas and Propagation 11(3):207–216
[21] Hunt K, Niemeier J, Kruger A (2010) RF communications in underwater wireless sensor networks. In: IEEE International Conference on Electro/Information Technology (EIT), Normal, IL
[22] Iizuka K (1964) An experimental investigation on the behavior of the dipole antenna near the interface between the conducting medium and free space. IEEE Transactions on Antennas and Propagation 12(1):27–35
[23] Johnson RC (ed) (1993) Antenna Engineering Handbook, 3rd edn. McGraw-Hill, Inc.
[24] Kesar AS, Weiss E (2013) Wave propagation between buried antennas. IEEE Transactions on Antennas and Propagation 61(12):6152–6156
[19] King RWP, Smith G (1981) Antennas in Matter. MIT Press

[20] King RWP, Owens M, Wu TT (1992) Lateral Electromagnetic Waves. Springer-Verlag
[20] Konda A, Rau A, Stoller MA, Taylor JM, Salam A, Pribil GA, Argyropoulos C, Morin SA (2018) Soft microreactors for the deposition of conductive metallic traces on planar, embossed, and curved surfaces. Advanced Functional Materials 28(40):1803020, DOI 10.1002/adfm.201803020
[28] Moore RK, Blair WE (1961) Dipole radiation in conducting half space. Journal of Res National Bureau of Standard 65
[26] Peplinski N, Ulaby F, Dobson M (1995) Dielectric properties of soil in the 0.3–1.3 ghz range. IEEE Transactions on Geoscience and Remote Sensing 33(3):803–807
[30] Ritsema CJ, etal (2009) A new wireless underground network system for continuous monitoring of soil water contents. Water Resources Research Journal 45:1–9
[24] Salam A (2018) Pulses in the sand: Long range and high data rate communication techniques for next generation wireless underground networks. ETD collection for University of Nebraska - Lincoln (AAI10826112), URL http://digitalcommons.unl.edu/dissertations/AAI10826112
[25] Salam A (2019) A comparison of path loss variations in soil using planar and dipole antennas. In: 2019 IEEE International Symposium on Antennas and Propagation, IEEE
[26] Salam A (2019) Design of subsurface phased array antennas for digital agriculture applications. In: Proc. 2019 IEEE International Symposium on Phased Array Systems and Technology (IEEE Array 2019), Waltham, MA, USA
[27] Salam A (2019) A path loss model for through the soil wireless communications in digital agriculture. In: 2019 IEEE International Symposium on Antennas and Propagation, IEEE, pp 1–2
[28] Salam A (2019) Sensor-free underground soil sensing. In: ASA, CSSA and SSSA International Annual Meetings (2019), ASA-CSSA-SSSA
[29] Salam A (2019) Subsurface mimo: A beamforming design in internet of underground things for digital agriculture applications. Journal of Sensor and Actuator Networks 8(3), DOI 10.3390/jsan8030041, URL https://www.mdpi.com/2224-2708/8/3/41
[30] Salam A (2019) Underground Environment Aware MIMO Design Using Transmit and Receive Beamforming in Internet of Underground Things, Springer International Publishing, Cham, pp 1–15
[33] Salam A (2019) An underground radio wave propagation prediction model for digital agriculture. Information 10(4), DOI 10.3390/info10040147, URL http://www.mdpi.com/2078-2489/10/4/147
[32] Salam A (2019) Underground soil sensing using subsurface radio wave propagation. In: 5th Global Workshop on Proximal Soil Sensing, Columbia, MO
[33] Salam A (2020) Internet of Things for Environmental Sustainability and Climate Change, Springer International Publishing, Cham, pp 33–69.

DOI 10.1007/978-3-030-35291-2_2, URL https://doi.org/10.1007/978-3-030-35291-2_2

[34] Salam A (2020) Internet of Things for Sustainability: Perspectives in Privacy, Cybersecurity, and Future Trends, Springer International Publishing, Cham, pp 299–327. DOI 10.1007/978-3-030-35291-2_10, URL https://doi.org/10.1007/978-3-030-35291-2_10

[35] Salam A (2020) Internet of Things for Sustainable Community Development, 1st edn. Springer Nature, DOI 10.1007/978-3-030-35291-2

[36] Salam A (2020) Internet of Things for Sustainable Community Development: Introduction and Overview, Springer International Publishing, Cham, pp 1–31. DOI 10.1007/978-3-030-35291-2_1, URL https://doi.org/10.1007/978-3-030-35291-2_1

[37] Salam A (2020) Internet of Things for Sustainable Forestry, Springer International Publishing, Cham, pp 147–181. DOI 10.1007/978-3-030-35291-2_5, URL https://doi.org/10.1007/978-3-030-35291-2_5

[38] Salam A (2020) Internet of Things for Sustainable Human Health, Springer International Publishing, Cham, pp 217–242. DOI 10.1007/978-3-030-35291-2_7, URL https://doi.org/10.1007/978-3-030-35291-2_7

[39] Salam A (2020) Internet of Things for Sustainable Mining, Springer International Publishing, Cham, pp 243–271. DOI 10.1007/978-3-030-35291-2_8, URL https://doi.org/10.1007/978-3-030-35291-2_8

[40] Salam A (2020) Internet of Things for Water Sustainability, Springer International Publishing, Cham, pp 113–145. DOI 10.1007/978-3-030-35291-2_4, URL https://doi.org/10.1007/978-3-030-35291-2_4

[41] Salam A (2020) Internet of Things in Agricultural Innovation and Security, Springer International Publishing, Cham, pp 71–112. DOI 10.1007/978-3-030-35291-2_3, URL https://doi.org/10.1007/978-3-030-35291-2_3

[42] Salam A (2020) Internet of Things in Sustainable Energy Systems, Springer International Publishing, Cham, pp 183–216. DOI 10.1007/978-3-030-35291-2_6, URL https://doi.org/10.1007/978-3-030-35291-2_6

[43] Salam A (2020) Internet of Things in Water Management and Treatment, Springer International Publishing, Cham, pp 273–298. DOI 10.1007/978-3-030-35291-2_9, URL https://doi.org/10.1007/978-3-030-35291-2_9

[44] Salam A (2020) Wireless underground communications in sewer and stormwater overflow monitoring: Radio waves through soil and asphalt medium. Information 11(2)

[46] Salam A, Karabiyik U (2019) A cooperative overlay approach at the physical layer of cognitive radio for digital agriculture. In: Third International Balkan

Conference on Communications and Networking 2019 (BalkanCom'19), Skopje, Macedonia, the former Yugoslav Republic of
[46] Salam A, Shah S (2019) Internet of things in smart agriculture: Enabling technologies. In: 2019 IEEE 5th World Forum on Internet of Things (WF-IoT), IEEE, pp 692–695
[139] Salam A, Vuran MC (2016) Impacts of soil type and moisture on the capacity of multi-carrier modulation in internet of underground things. In: Proc. ICCCN 2016, Waikoloa, Hawaii, USA
[47] Salam A, Vuran MC (2016) Impacts of soil type and moisture on the capacity of multi-carrier modulation in internet of underground things. In: Proc. of the 25th ICCCN 2016, Waikoloa, Hawaii, USA
[48] Salam A, Vuran MC (2017) Em-based wireless underground sensor networks pp 247–285, DOI 10.1016/B978-0-12-803139-1.00005-9
[49] Salam A, Vuran MC (2017) Smart underground antenna arrays: A soil moisture adaptive beamforming approach. In: Proc. IEEE INFOCOM 2017, Atlanta, USA
[50] Salam A, Vuran MC (2017) Wireless underground channel diversity reception with multiple antennas for internet of underground things. In: Proc. IEEE ICC 2017, Paris, France
[145] Salam A, Vuran MC, Irmak S (2016) Pulses in the sand: Impulse response analysis of wireless underground channel. In: Proc. IEEE INFOCOM 2016, San Francisco, USA
[51] Salam A, Vuran MC, Irmak S (2016) Pulses in the sand: Impulse response analysis of wireless underground channel. In: The 35th Annual IEEE International Conference on Computer Communications (INFOCOM 2016), San Francisco, USA
[61] Salam A, Vuran MC, Irmak S (2016) Pulses in the sand: Impulse response analysis of wireless underground channel. In: The 35th Annual IEEE International Conference on Computer Communications (INFOCOM 2016), San Francisco, USA
[62] Salam A, Vuran MC, Irmak S (2017) Towards internet of underground things in smart lighting: A statistical model of wireless underground channel. In: Proc. 14th IEEE International Conference on Networking, Sensing and Control (IEEE ICNSC), Calabria, Italy
[52] Salam A, Vuran MC, Irmak S (2017) Towards internet of underground things in smart lighting: A statistical model of wireless underground channel. In: Proc. 14th IEEE International Conference on Networking, Sensing and Control (IEEE ICNSC), Calabria, Italy
[53] Salam A, Hoang AD, Meghna A, Martin DR, Guzman G, Yoon YH, Carlson J, Kramer J, Yansi K, Kelly M, et al. (2019) The future of emerging iot paradigms: Architectures and technologies
[54] Salam A, Vuran MC, Dong X, Argyropoulos C, Irmak S (2019) A theoretical model of underground dipole antennas for communications in internet of underground things. IEEE Transactions on Antennas and Propagation

[66] Salam A, Vuran MC, Dong X, Argyropoulos C, Irmak S (2019) A theoretical model of underground dipole antennas for communications in internet of underground things. IEEE Transactions on Antennas and Propagation 67(6):3996–4009

[55] Salam A, Vuran MC, Irmak S (2019) Di-sense: In situ real-time permittivity estimation and soil moisture sensing using wireless underground communications. Computer Networks 151:31 – 41, DOI https://doi.org/10.1016/j.comnet.2019.01.001, URL http://www.sciencedirect.com/science/article/pii/S1389128618303141

[68] Salam A, Vuran MC, Irmak S (2019) Di-sense: In situ real-time permittivity estimation and soil moisture sensing using wireless underground communications. Computer Networks 151:31 – 41, DOI https://doi.org/10.1016/j.comnet.2019.01.001, URL http://www.sciencedirect.com/science/article/pii/S1389128618303141

[61] Silva AR, Vuran MC (2010) $(CPS)^2$: integration of center pivot systems with wireless underground sensor networks for autonomous precision agriculture. In: Proc. of ACM/IEEE International Conf. on Cyber-Physical Systems, Stockholm, Sweden, pp 79–88, DOI http://doi.acm.org/10.1145/1795194.1795206

[70] Sivaprasad K, King R (1963) A study of arrays of dipoles in a semi-infinite dissipative medium. Antennas and Propagation, IEEE Transactions on 11(3):240–256, DOI 10.1109/TAP.1963.1138045

[67] Staiman D, Tamir T (1966) Nature and optimisation of the ground (lateral) wave excited by submerged antennas. Electrical Engineers, Proceedings of the Institution of 113(8), DOI 10.1049/piee.1966.0220

[72] Tai CT, Collin RE (2000) Radiation of a hertzian dipole immersed in a dissipative medium. IEEE Transactions on Antennas and Propagation 48(10):1501–1506

[65] Temel S, Vuran MC, Lunar MM, Zhao Z, Salam A, Faller RK, Stolle C (2018) Vehicle-to-barrier communication during real-world vehicle crash tests. Computer Communications 127:172–186

[74] Tiusanen MJ (2008) Wireless Soil Scout prototype radio signal reception compared to the attenuation model. Precision Agriculture 10(5):372–381

[75] Vuran MC, Salam A, Wong R, Irmak S (2018) Internet of underground things in precision agriculture: Architecture and technology aspects. Ad Hoc Networks DOI https://doi.org/10.1016/j.adhoc.2018.07.017, URL http://www.sciencedirect.com/science/article/pii/S1570870518305067

[76] Vuran MC, Salam A, Wong R, Irmak S (2018) Internet of underground things in precision agriculture: Architecture and technology aspects. Ad Hoc Networks DOI https://doi.org/10.1016/j.adhoc.2018.07.017, URL http://www.sciencedirect.com/science/article/pii/S1570870518305067

[72] Vuran MC, Salam A, Wong R, Irmak S (2018) Internet of underground things: Sensing and communications on the field for precision agriculture. In: 2018 IEEE 4th World Forum on Internet of Things (WF-IoT) (WF-IoT 2018), , Singapore

[78] Wait JR (1961) The electromagnetic fields of a horizontal dipole in the presence of a conducting half-space. Canadian Journal of Physics 39(7):1017–1028

[79] Wheeler HA (1961) Useful radiation from an underground antenna. Journal of Research 65:89–91

[80] Zemmour H, Baudoin G, Hamouda C, Diet A, Biancheri-Astier M (2015) Impact of soil on uwb buried antenna and communication link in ir-uwb wusn applications. In: Radar Conference (EuRAD), 2015 European, pp 353–356, DOI 10.1109/EuRAD.2015.7346310